

RESEARCH ARTICLE | MAY 20 2002

Room-temperature homogeneous nucleation synthesis and thermal stability of nanometer single crystal CeO_2

X.-D. Zhou; W. Huebner; H. U. Anderson

*Appl. Phys. Lett.* 80, 3814–3816 (2002)<https://doi.org/10.1063/1.1481244>

Articles You May Be Interested In

Size-induced lattice relaxation in CeO_2 nanoparticles*Appl. Phys. Lett.* (November 2001)

Photoconductive properties of nanometer-sized Si dot multilayers

Appl. Phys. Lett. (October 2001)

Fabrication of nanometer-spaced superconducting Pb electrodes

Appl. Phys. Lett. (September 2009)

Applied Physics Letters

Special Topics Open for Submissions

[Learn More](#)

Room-temperature homogeneous nucleation synthesis and thermal stability of nanometer single crystal CeO₂

X.-D. Zhou,^{a)} W. Huebner, and H. U. Anderson

Electronic Materials Applied Research Center, Department of Ceramic Engineering, University of Missouri-Rolla, Rolla, Missouri 65401

(Received 5 February 2002; accepted for publication 24 March 2002)

Nanometer (about 4–5 nm) CeO₂ single crystals were first synthesized by room-temperature homogeneous nucleation; the size was determined by electron microscopy and specific surfaced area of the particles. Modeling revealed that the surface energy of as-synthesized nanometer single crystals was in the range of 2.8–3.7 J/m². Crystal growth mechanisms change over the temperature regimes, from boundary diffusion over low-temperature regime ($E_a=0.16$ eV) to bulk diffusion ($E_a=0.50$ eV) over high-temperature region. © 2002 American Institute of Physics. [DOI: 10.1063/1.1481244]

Nanometer cerium dioxide (CeO₂) particles have been of great interest because of the significant size-induced property changes, such as the Raman-allowed modes shifting and broadening;^{1,2} the lattice expansion;³ the pressure-induced phase transformation;⁴ the blue shift in ultraviolet absorption spectra.⁵ Very recently, we reported that lattice expansion of nanometer CeO₂ single crystals was attributed to the higher defect concentrations of Ce³⁺ and oxygen vacancies (V_O^\bullet)⁶ and the influences of the porosity on the changes of optical absorption in the porous films prepared from nanometer CeO₂ colloidal solutions.⁷ Moreover, nanocrystalline CeO₂ particles allowed a sintering temperature of 1000 °C, which is 200–400 °C lower than that reported for microcrystalline particles.⁸ In order to investigate the properties of nanocrystalline CeO₂, it is extremely important to be able to synthesize nanometer free surface particles with a narrow size distribution and an average size about 4–5 nm.⁹

It is the intent of this letter to describe a method for the synthesis of the nanometer single crystals, in which the crystal size was tailored in a semibatch reactor with control over the homogeneous nucleation and growth mechanisms achieved by high speed mixing with an impeller. In this case a high purity cerium nitrate solution was added into an aqueous ammonium hydroxide precipitant. Oxygen was bubbled into the reactor with passage through a gas distributor to oxidize the Ce³⁺ to Ce⁴⁺. The as-synthesized particles were yellow with the flow of oxygen whereas purple products were achieved without oxygen, which shows the possible mixture of Ce³⁺ and Ce⁴⁺ compounds. Moreover, the particle size is smaller when oxygen bubble was used.⁸ Excessive precipitant was used so that the pH value was ≈ 9 after the reaction was complete. Precipitates were dried at room temperature and directly yielded CeO₂ particles.

Figure 1 shows the pH value evolution during the precipitation process; the pH value always remained higher than 9 (i.e., $[\text{OH}^-]$ higher than 10^{-5} mol/l). The primary particle size is ≈ 4 nm as determined from transmission electron microscopy (TEM). Under these basic conditions, the solubility

product is much higher than the solubility constant, meaning the supersaturation value (S) is very large.

$$S = \frac{[\text{Ce}^{3+}][\text{OH}^-]^3}{K_{\text{SP}}}, \quad (1)$$

where K_{SP} is the solubility constant of Ce(OH)₃.

A high supersaturation value, S , establishes an environmental condition that favors homogeneous nucleation. Homogeneous nucleation typically results in the formation of uniform nuclei with a critical size which can be calculated from:¹⁰

$$r^* = \frac{2v\gamma}{k_B T \ln(S)}, \quad (2)$$

where: v =molecular volume of the precipitated embryo (m³), γ =surface energy (J/m²), k_B =Boltzmann constant (J/K), T =temperature (K), S =supersaturation value.

The density ρ of Ce(OH)₃ was calculated to be 4.752 g/cm³ from the tabulated lattice parameters.¹¹ Hence where MW is molecular weight and N_A is the Avogadro constant $v = MW_{\text{Ce(OH)}_3} / (N_A \rho) = 6.68 \times 10^{-29}$ m³. The solubility constant, K_{sp} , of various hydroxides have been calculated from thermodynamic data¹² and measured experimentally.¹³ For precipitation process in this research, the precipitant had

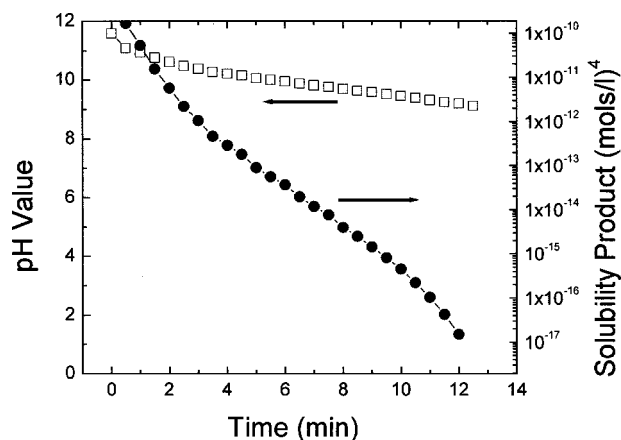
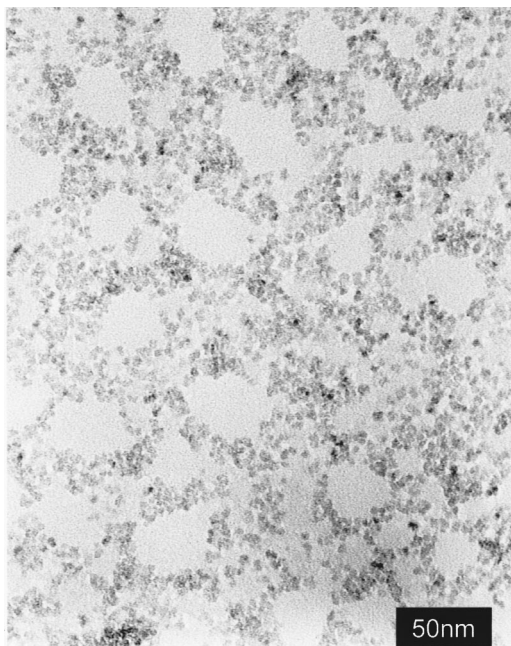


FIG. 1. pH and solubility product changes during the precipitation process.

^{a)}Author to whom correspondence should be addressed; electronic mail: Zhou@umr.edu

FIG. 2. TEM image of the CeO₂ particles.

a pH=12, therefore the $[\text{OH}^-] = 10^{-2}$ moles/l. The starting $[\text{Ce}^{3+}]$ in the nitrate solution was 10^{-1} moles/l. Some question related to the “local” $[\text{Ce}^{3+}]$ will exist however, since there is no way of knowing for sure over what volume it diffused in the precipitant during the precipitation process. If it completely diffused in the reactor volume, the $[\text{Ce}^{3+}] = 10^{-4}$ mole/l, corresponding to $S = 1.4 \times 10^{10}$; whereas $S = 1.4 \times 10^{13}$ in the case of complete segregation of Ce^{3+} . In the case of adding ammonium aqueous solution into cerium nitrate solution, the solubility product, $[\text{Ce}^{3+}][\text{OH}^-]^3$, is less than the critical solubility constant of $\text{Ce}(\text{OH})_3$, due to a low pH value of cerium nitrate solution (pH \approx 3.8). Under these conditions then, even though a nucleus may form at the interface, it is in an unstable state because of the low pH value of the bulk solution. The redissolution process is called ripening, which resulted in the particle with random size and morphology.

In this work the primary particle size was constant over a wide of range of experimental precipitation conditions, supporting the assumption that homogeneous nucleation took place. Figure 2 is the image of the particles after only a 1 s

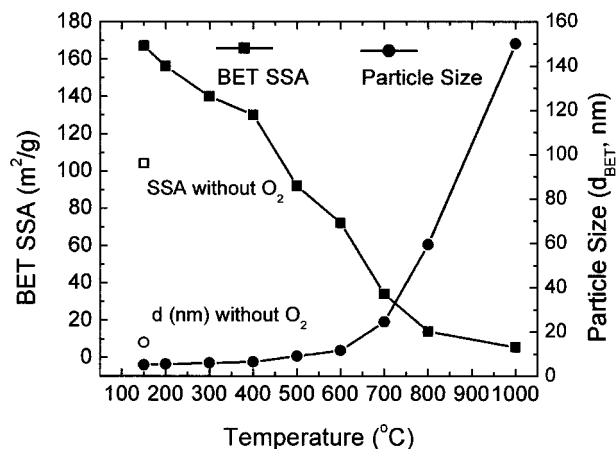


FIG. 3. The variation of the specific surface area and particle size over various annealing temperatures of nanometer CeO₂ from the process with oxygen bubbles. The data of CeO₂ nanometer particles without oxygen are also shown as the hollow symbols.

precipitation process; again the crystallite size is ≈ 4 nm. From Eq. (2) then, the surface energy of the crystallites was calculated to be in the range of 2.8–3.7 J/m².

The nanometer scale particle size of the CeO₂ prepared in this work is advantageous for applications where a fine particle size is necessary (e.g., catalysts), and should allow for lower sintering temperature. Hence, how these powders coarsen with annealing temperature is of interest. Figure 3 shows the specific surface area (SSA, m²/g) measured by the Brunauer–Emmett–Teller (BET) method and corresponding particle size for annealing temperatures ranging from 150 to 1000 °C, all for a 1 h anneal time. The particle size (d_{BET} , μm) was calculated from the specific surface area data by assuming spherical particles with the relationship of $d_{\text{BET}} = 6/(\rho \cdot \text{SSA})$, using a value of the density for particles. The particle size slowly increased up to 500 °C, rapidly increased for temperatures greater than 600 °C, and achieved a size of 100 nm at 1000 °C. The specific surface area in this study is higher than that of CeO₂ supported catalysts from literature.¹⁴ An Arrhenius plot of these data (Fig. 4) revealed an interesting observation; two distinctly linear regions are apparent. Very recently, a similar behavior was observed for nanometer ZrO₂ particles,⁹ in which a model of $D(T) = D_0 \exp(-E_a(T)/T)$ was proposed, where D is the particle size; $E_a(T)$ is the temperature dependent activation energy; T is the temperature, and $E_a(T)/T$ is shown in Eq. (3):

$$\frac{E_a(T)}{T} = \frac{(E_{a1} + E_{a2})\left(\frac{1}{T} - \frac{1}{T_0}\right) - \left\{ \left[(E_{a1} - E_{a2})\left(\frac{1}{T} - \frac{1}{T_0}\right) \right]^2 + 4\Delta^2 \right\}^{1/2}}{2}. \quad (3)$$

In this relation, E_{a1} and E_{a2} are activation energies for the high and low temperature regimes, respectively; T_0 and Δ represent, respectively, the temperature and the width of the transition. The activation energy ($E_a \sim 0.16$ eV) in the low temperature range was much smaller than that ($E_a \sim 0.50$ eV) in the high temperature region; the width of the transition (Δ) was about 0.2, which showed a relatively wide

transition window. The mechanism behind this behavior is not clear. Previous work⁶ showed a TEM lattice image of a collection of CeO₂ primary particles after room temperature drying. Many crystalline particles were observed (supporting the x-ray diffraction data), but a large fraction of the ensemble appeared to be disordered, perhaps even amorphous on the surface of the crystallite. The transition from amor-

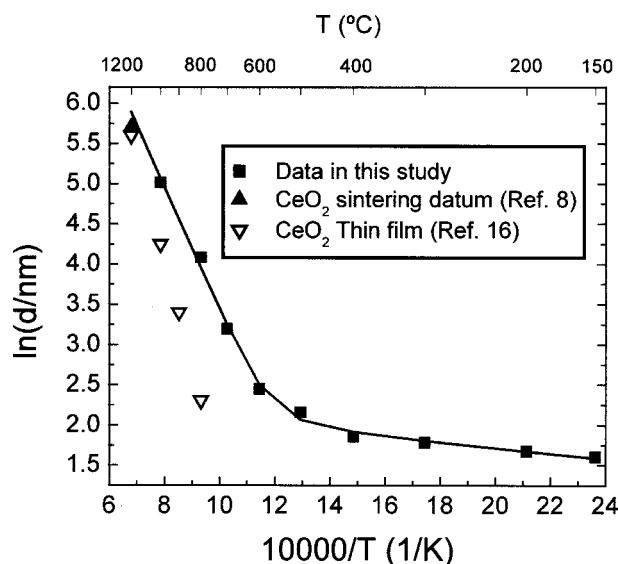


FIG. 4. Arrhenius plots of the variation of nanometer CeO₂ particle size over various annealing temperatures.

phous to crystallite state provides a large driving force for diffusion and subsequent growth at higher temperatures. Simple atomic rearrangement and ordering can result in a slow increase in particle size. Typically boundary diffusion has a lower activation energy than the other mechanisms,^{10,15} so it is possible this is the dominant mechanism at low temperatures. At higher annealing temperatures bulk diffusion controls the particle size evolution because of the higher activation energy associated with long range ordering and particle rearrangement. Grain growth over the high temperature regime in thin CeO₂ films¹⁶ exhibits a similar behavior, which is also shown in Fig. 4; the activation energy was around 1.1 eV for thin film, whereas only ~ 0.50 eV for nanocrystal growth.

In conclusion, nanometer (about 4–5 nm) CeO₂ single crystals were synthesized by homogeneous nucleation at

room temperature by careful control of the solubility products and the oxidation rate. Nanocrystal sizes were determined by electron microscopy and specific surfaced area of as-synthesized particles. Modeling revealed that the surface energy of as-synthesized nanometer crystallites was in the range of 2.9 to 3.7 J/m². Crystal growth mechanisms change over the temperature regimes, perhaps from boundary diffusion controlled over the low temperature region to lattice diffusion at higher temperatures.

We acknowledge the support by the U.S. Department of Energy under Contract No. DE-A26-99FT46710.

- ¹W. H. Weber, K. C. Hass, and J. R. McBride, Phys. Rev. B **50**, 13 297 (1993).
- ²J. E. Spanier, R. D. Robinson, F. Zhang, S.-W. Chan, and I. Herman, Phys. Rev. B **64**, 245407 (2001).
- ³S. Tsunekawa, K. Ishikawa, Z.-Q. Li, Y. Kawazoe, and A. Kasuya, Phys. Rev. Lett. **85**, 3440 (2000).
- ⁴Z. Wang, S. K. Saxena, V. Pischedda, H. P. Liermann, and C. S. Zha, Phys. Rev. B **64**, 012102 (2001).
- ⁵S. Tsunekawa, T. Fukuda, and A. Kasuya, J. Appl. Phys. **87**, 1318 (2000).
- ⁶X.-D. Zhou and W. Huebner, Appl. Phys. Lett. **79**, 3512 (2001).
- ⁷V. Petrovsky, B. P. Gorman, H. U. Anderson, and T. Petrovsky, J. Appl. Phys. **90**, 2517 (2001).
- ⁸X.-D. Zhou, Ph.D. dissertation, University of Missouri-Rolla, 2001.
- ⁹M. Jouanne, J. F. Morhange, M. A. Kanehisa, E. Haro-Poniatowski, G. A. Fuentes, E. Torres, and E. Hernández-Tellez, Phys. Rev. B **64**, 155404 (2001).
- ¹⁰J. A. Dirksen and T. A. Ring, Chem. Eng. Sci. **46**, 2389 (1991).
- ¹¹D. F. Mullica, J. D. Oliver and W. O. Milligan, Acta Crystallogr., Sect. B: Struct. Crystallogr. Cryst. Chem. **35**, 2668 (1979).
- ¹²C. F. Baes, Jr. and R. E. Mesmer, *The Hydrolysis of Cations* (Wiley, New York, 1976).
- ¹³T. Moeller and H. E. Kremers, J. Chem. Phys. **48**, 395 (1944).
- ¹⁴B. Bernal, F. J. Botana, J. J. Calvino, M. A. Cauqui, G. A. Cifredo, A. Jobacho, J. M. Pintado, and J. M. Rodriguez-Izquierdo, J. Phys. Chem. **97**, 4118 (1993).
- ¹⁵J. H. Harding and D. J. Harris, Phys. Rev. B **63**, 094102 (2001).
- ¹⁶T. Suzuki, I. Kosacki, H. U. Anderson, and P. Colomban, J. Am. Ceram. Soc. **84**, 2007 (2001).